



New polymeric matrix of polylactic acid/sodium alginate/carbon nanoparticles (PLA/SA/CNP) for efficient removal of methylene blue

Reem Fathy¹ · Eman Ragab¹ · Korany A. Ali²

Received: 9 January 2023 / Accepted: 14 June 2023 / Published online: 19 July 2023
© The Author(s) 2023

Abstract

For the adsorption of methylene blue (MB), novel bio-polymeric matrices prepared from polylactic acid/sodium alginate (PLA/SA) and polylactic acid/sodium alginate/carbon nanoparticle (PLA/SA/CNP) as green adsorbates were prepared in the form of beads. The developed adsorbent was analyzed using scanning electron microscopes and Fourier transform infrared spectrometers. The percentage of adsorbed dye increased with increasing CNP content, and the optimum ratio was 5% wt. The efficiency of the beads' removal and adsorption capacity were evaluated concerning with (adsorbent dosage, contact time, initial pH, and concentration of adsorbate). After 120 min using 50 mg of PLA/SA/CNP beads, the adsorptive removal process for MB dye was determined to have the maximum rate at pH 9. The models of Langmuir and Freundlich were used to illustrate the experimental data. Langmuir models determined the highest adsorption capacity to be 304.88 mg/g.

Keywords Wastewater treatment · Bio-polymeric matrix · Polylactic acid · Carbon nanoparticle · Methylene blue

Introduction

Dyes are used in various industrial processes, including the dyeing, textile, paint, cosmetics, paper printing, and plastics sectors (Labena et al. 2021; Sattar et al. 2017). Dye is a crucial part of several manufacturing processes. Most dyes are resistant to light, heat, oxidizing chemicals and are not biodegradable. As a result, their presence in wastewater in large numbers causes significant environmental harm (Ho et al. 2020).

One of the significant contributors to water pollution is the large volume of industrial effluents produced, which are harmful to aquatic species and humans. For example, in the textile industry, more than 200,000 tons of dyes are lost due to inefficiencies in this process. Furthermore, several dye's degradation products may be toxic, mutagenic, or carcinogenic, producing extra pollution to the ecosystem (Sattar et al. 2017). Due to their complex structures, dye-induced

color in effluents also contributes significantly to pollution in aquatic habitats (Sumanjit and Kaur 2007), where they collect in the water and prevent bacterial growth and photosynthesis by absorbing sunlight as it enters the biosphere. According to the dye content (Labena et al. 2021) and exposure duration, dyes also have various long-term effects on organisms (Sumanjit and Kaur 2007; Amin et al. 2010). The ingestion and dye exposure is connected to several health issues (Wan et al. 2011). Dye removal has gained great attention and needs a lot of work because dye presence in wastewater poses several risks (Wan et al. 2011). These include ion exchange (Wan et al. 2011). Electrochemical, advanced oxidation process, chemical oxidation, biological process, membrane filtration (Li et al. 2008), photocatalysis (Koumanova and Allen 2005), and adsorption (Sabarinathan et al. 2019) (Wan et al. 2011). The advantages of the adsorption technique are low cost, ease of application, ease of design, effectiveness, and the ability to reuse and regenerate adsorbents (Annadurai et al. 1999; McKay et al. 1986; and Ayad et al. 2012). Additionally, the capacity to modify the adsorbent's surface, which permits increased adsorbent performance, is a significant advantage of the adsorption process (Annadurai et al. 1999). To increase removal efficiency, selectivity, and longevity, a number of modified materials have been developed (Koumanova and Allen 2005).

✉ Korany A. Ali
kornykhilil@gmail.com; ka.khalil@nrc.sci.eg

¹ Department of Chemistry, Faculty of Science, Cairo University, Cairo, Egypt

² Applied Organic Chemistry Department, Center of Excellence for Advanced Science, National Research Centre, Giza 12622, Egypt

Agricultural waste, clay minerals (McKay et al. 1986) and zeolites chitosan, and chitin (Annadurai et al. 1999) are some of these adsorbents, as well as carbon-based substances such multi-walled nanotubes, (Makhado and Hato 2021), activated carbons, and graphene oxide (Song et al. 2022) (Ayad et al. 2012). The use of the above materials is still constrained by their partial adsorption capability, low reusability, the large volume of sludge production, and high operating costs (Crini and Badot 2008). The most frequently used adsorbents are activated carbon (Wang et al. 2020) and polymers (Salisu et al. 2015; Mohammad and Atassi 2020; Ali et al. 2017). Carbon nanoparticles have generated a lot of interest recently due to their advantages, including their high adsorption capacity, large surface area, high porosity, and thermal stability, which make them a flexible adsorbent with high adsorption effectiveness and suitable for wastewater treatment (Abdel Moniem et al. 2022). CNP is a non-graphite form of carbon that can be made from activated carbon materials such as coconut shells, bamboo, wood chips, sawdust, and other agricultural wastes. Due to their biodegradability, affordability, and availability, biomaterials, in particular biopolymers made from renewable sources, can be employed as an alternative to conventional adsorbents (Kaushal and Tiwari 2010).

PLA is a biodegradable thermoplastic aliphatic polyester derived from renewable resources including tapioca roots, maize starch, chips, and starch (Mohammad and Atassi 2020) and its structure is shown in Fig. 1. Alginate is a polymer derived from brown algae found in seaweed (Ali et al. 2017) (Soleimani et al. 2023) composed mainly from the residue of β -1,4-linked-D-mannuronic acid (M-Block) and α -1,4-linked-L-guluronic acid (G-Block) Fig. 1. Alginate's use in recovering valuable metals and eliminating hazardous elements has been extensively investigated (Ali et al. 2017). The alginate was previously used to remove Rhodamine-B from an aqueous solution utilizing adsorption onto cross-linked alginate beads and to extract methylene blue from an aqueous solution using magnetic alginate beads cross-linked with epichlorohydrin (Hu, T. et al. 2018). (Kaushal and Tiwari 2010).

Based on these findings and in keeping with our ongoing research in this area, we have designed and developed a novel polymeric matrix of PLA/SA/CNP beads for the adsorption of methylene blue (MB). The effectiveness of

removing methylene blue from the porous beads was then evaluated in an aqueous media as a model for the future treatment of industrial colors in wastewater.

Experimental

Chemicals

Poly(lactic acid) (PLA) (Ingeo^{T M} 6202D fiber grade) was purchased from nature works LLC (USA). Sodium alginate (ALG- Na^+), carbon nanoparticle (CNP) and methylene blue (MB) were purchased from Sigma-Aldrich (Germany). CaCl_2 were purchased from Elnaser for the chemical industry-Egypt. All the other reagents were in the analytical grade and were used without further purification.

Instrumentation

A UV–vis spectrophotometer was used to measure dye concentration (Chrom Tech, Ltd, USA) A magnetic stirrer (VELP, SCIENTIFIC, Italy), and analytical balance (Mettler AJ150) and GALLENKAMP (flask Shaker, five speeds) were used. The pH was determined using the Jenway pH Metre 3310. The Nicolet i10 FT-IR spectrometer from Thermofisher Scientific, USA, was used to investigate FTIR spectra in the region of ($4000\text{--}500\text{ cm}^{-1}$). SEM was used to characterize the surface structure morphology of the ALG/PLA/CNP composite beads using a Quanta 250 FEG model (Field Emission Gun).

Preparation of adsorbate (MB dye)

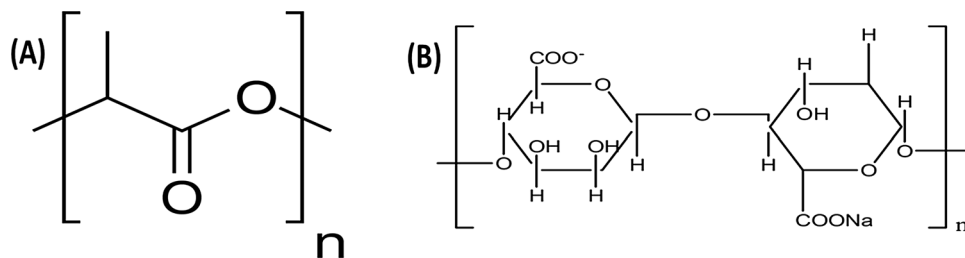
A 1000 mg/L stock solution was prepared by dissolving 1.00 g of MB dye in 1000 mL of distilled water. Different concentrations of MB dye were prepared using appropriate dilutions of the stock solution (Fig. 2).

Preparation of adsorbent (PLA/SA/CNP beads)

Preparation of PLA/SA beads

PLA/SA beads were prepared by dissolving 2 g SA in 100 mL distilled water for 4 h with stirring at room

Fig. 1 The chemical structure of poly(lactic acid) (PLA) (a), and sodium alginate (SA) (b)



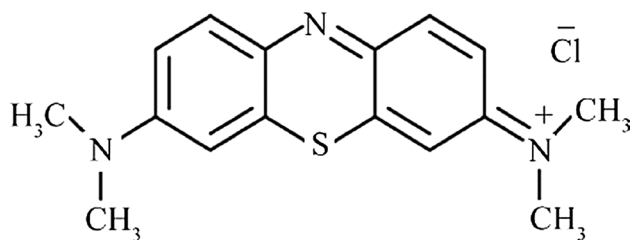


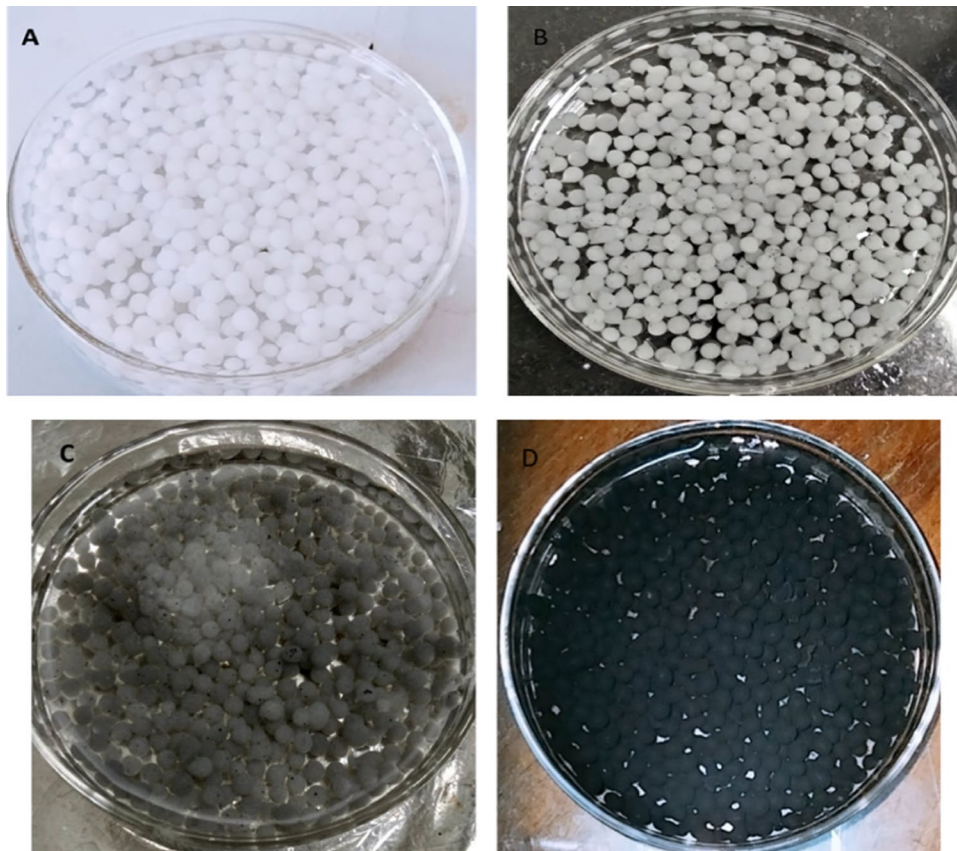
Fig. 2 The chemical structure of methylene blue (MB)

temperature and 1 g PLA in 100 mL acetone for 24 h with stirring at room temperature. Then the SA solution was added drop by drop to the PLA solution. The PLA/SA beads were created by dropping the PLA/SA solution into a magnetically stirred 3% (w/v) CaCl₂ solution using a syringe with a needle (1.2 × 38 mm), which resulted in solid beads as illustrated in Fig. 3.

Preparation of PLA/SA/CNP beads

PLA/SA/CNP beads as shown in Fig. 3 were prepared, as mentioned previous step in addition to adding different weights (1, 3, 5) wt% of CNP.

Fig. 3 Camera picture of beads **a** PLA/SA, **b** PLA/SA/1% wt CNP, **c** PLA/SA/3% wt CNP, and **d** PLA/SA/5% wt CNP



Batch adsorption experiments

100-mL Erlenmeyer flasks were filled with a particular number of beads and 50 mL of dye aqueous solution, and they were violently shaken in a temperature-controlled water bath shaker utilizing the variable initial dye concentration (50–200 mg/L), pH range (3–10), temperature (25 C), doses (20–200 mg) and duration of contact (15–120 min). At 663 nm, the concentration of the solution's un-adsorbed (remaining) MB dye was measured spectrophotometrically. The following equations were used to determine the adsorption capacity and percentage removal of MB dye by the adsorbent:

$$q_e(\text{mg/g}) = \frac{V(C_0 - C_e)}{m} \quad (1)$$

$$\text{Removal \%} = \frac{(C_0 - C_e)}{C_0} 100 \quad (2)$$

where q_e (mg/g) capacity of adsorption, C_0 (mg/L) and C_e (mg/L) are the initial and equilibrated concentrations of MB dye, respectively, V (L) is the total solution volume and m (g) dry mass of the adsorbent.

Results and discussion

The microbeads construction achieved by hydrogen bonding interaction between PLA and SA followed by crosslinking by CaCl_2 to form the uniform beads. Figure 4 shows the proposed mechanism for reactions.

Characterization of adsorbent

FTIR spectra

FTIR spectrum in the range of ($4000\text{--}500\text{ cm}^{-1}$) of the prepared adsorbent was taken to detect the functional groups responsible for the adsorption process and illustrated in Fig. 5. It is noticeable in curve CNP that the characteristic peak at 1500 cm^{-1} is associated with the $\text{C}=\text{C}$. For the PLA curve, it is observed the characteristic peak at 1752 cm^{-1} is related to the $\text{C}=\text{O}$ group. Other prominent peaks at 1085 and 1183 cm^{-1} represent $\text{C}-\text{O}$ stretching for $\text{C}-\text{O}-\text{C}$ and $\text{C}-\text{O}$, respectively. $\text{C}-\text{H}$ bending is illustrated by peaks at 1382 cm^{-1} and 1453 cm^{-1} for CH_3 and $\text{CH}=\text{CH}_3$, similar results (Ho et al. 2020). In Fig. 5, abroad peak at around 3446 cm^{-1} related to the stretching vibration of the hydroxyl groups present in SA polymer. The peak observed at 1600 , 1407 and 1034 cm^{-1} was ascribed to COO^- , $\text{C}-\text{C}$ band vibration and $\text{C}-\text{O}-\text{C}$, respectively, in the PLA/SA copolymer chain. The peak at $2,925\text{ cm}^{-1}$ corresponded to the $-\text{CH}_2-$ stretching vibrations of the CH_2 . The peak at 1600 cm^{-1} is due to COO^- groups. The peak at 1416 cm^{-1} is due to the $\text{C}-\text{C}$ bending vibration. The characteristic peak at 1030 cm^{-1} is related to the $\text{C}-\text{O}-\text{C}$ stretching frequencies. The characteristic bands correspond to $\text{Na}-\text{O}$ at 818 cm^{-1} . It was observed from the curve PLA/SA/CNP, Fig. 5, and the characteristic peaks at 2922 and 2852 cm^{-1} are associated

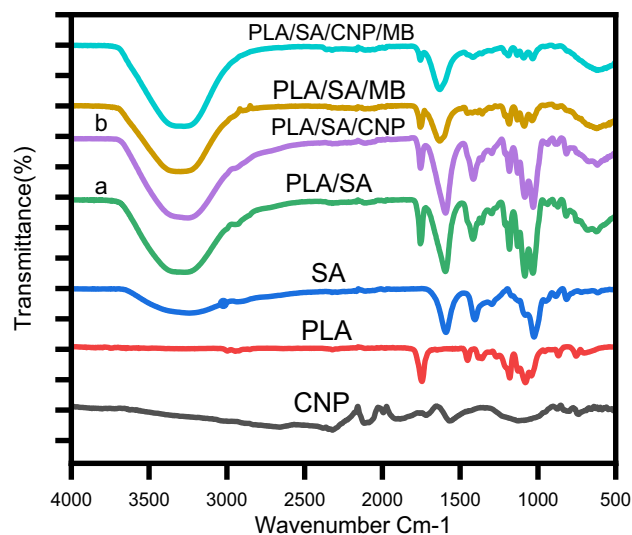


Fig. 5 FTIR of the prepared adsorbent a PLA/SA, and b PLA/SA/CNP

with the CH_2 group's asymmetric stretching and symmetric vibrations.

Scanning Electron Microscopy (SEM)

SEM used to examine and describe the prepared beads' surface (SEM). At various magnifications, SEM images of all the beads shown in Fig. 6. It observed that the beads were spherical in shape. The average particle size of the PLA/SA beads was $2.547\text{ }\mu\text{m}$. However, the PLA/SA/CNP beads $3.018\text{ }\mu\text{m}$ are shown in Fig. 6a, c. It is noticeable that there is a slight increase in size may have resulted from added of CNP to the beads. After the addition of CNP to the PLA/SA beads, there may have been some molecular interaction

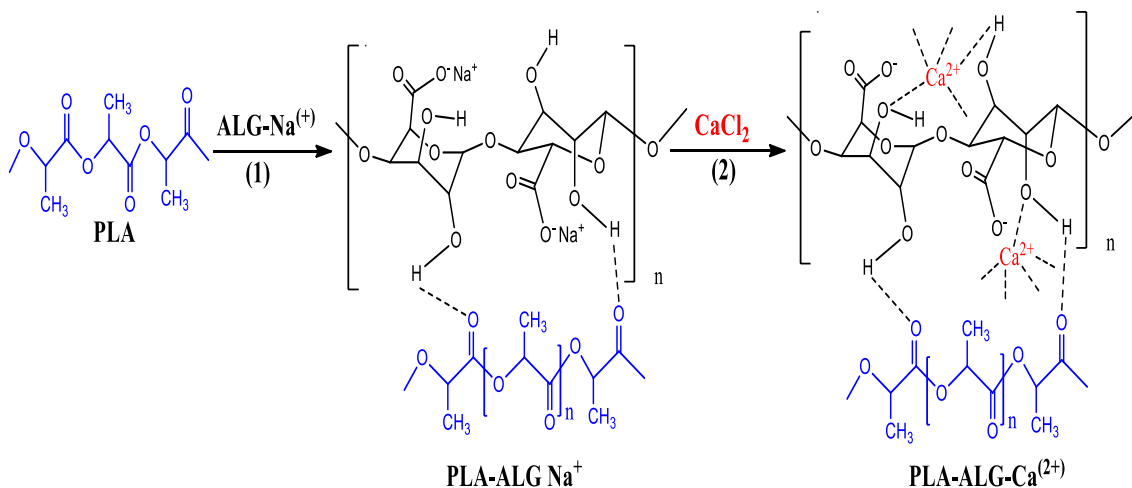
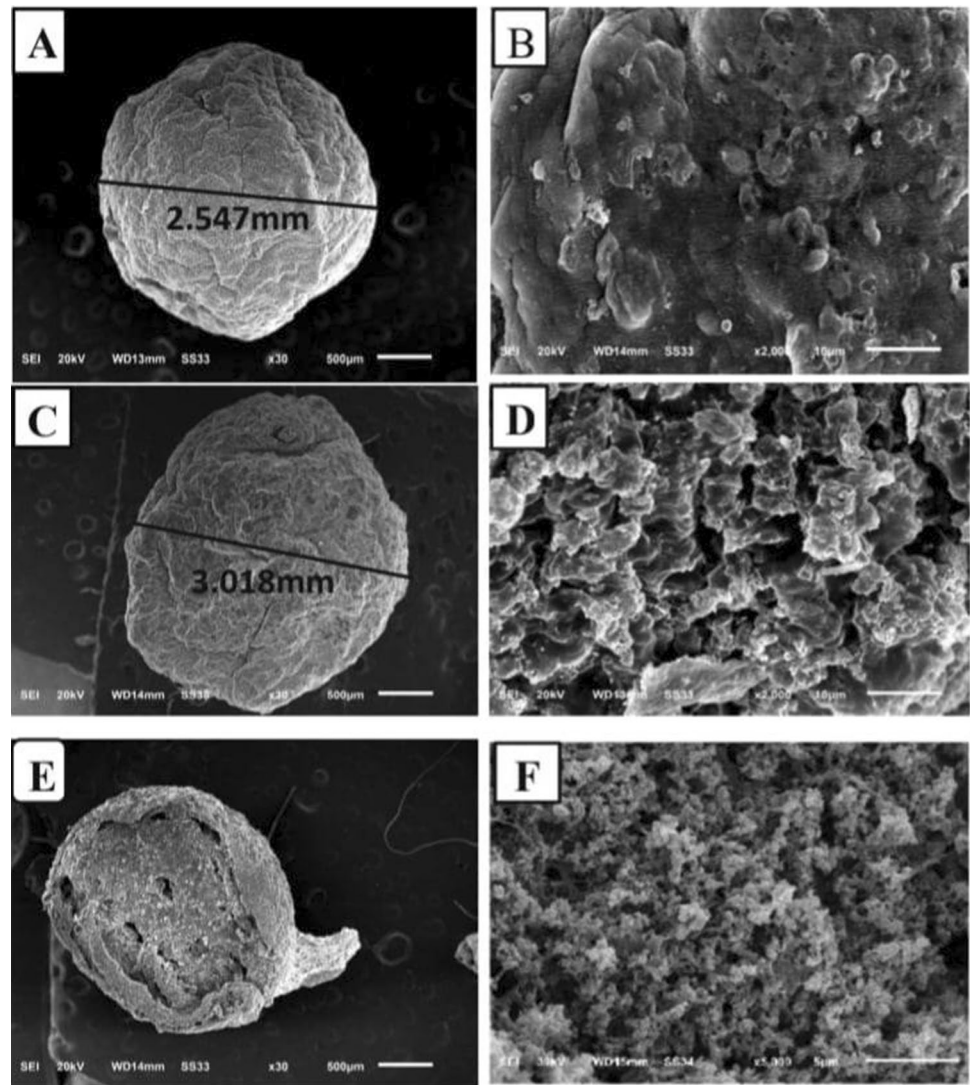


Fig. 4 The reactions involved in the preparation of composite PLA-ALG- Ca^{2+}

Fig. 6 SEM image of **a, b** PLA/SA, **c, d** PLA/SA/CNP and **e, f** cross-sectional of PLA/SA/CNP beads



between those polymers, and this may have caused a better porous surface of the beads and the structural changes in the morphology of the beads as illustrated in Fig. 6b, c. The cross-sectional SEM images of PLA/SA/CNP are presented in Fig. 6e, f. Figure 6f illustrates that the granules' surface was particularly porous, offering additional potential locations for the adsorption of metal ions. Because of the alginate activated carbon's porous structure, which provides enough surface for the adsorption of dye.

pH at a zero-point charge (pHzpc)

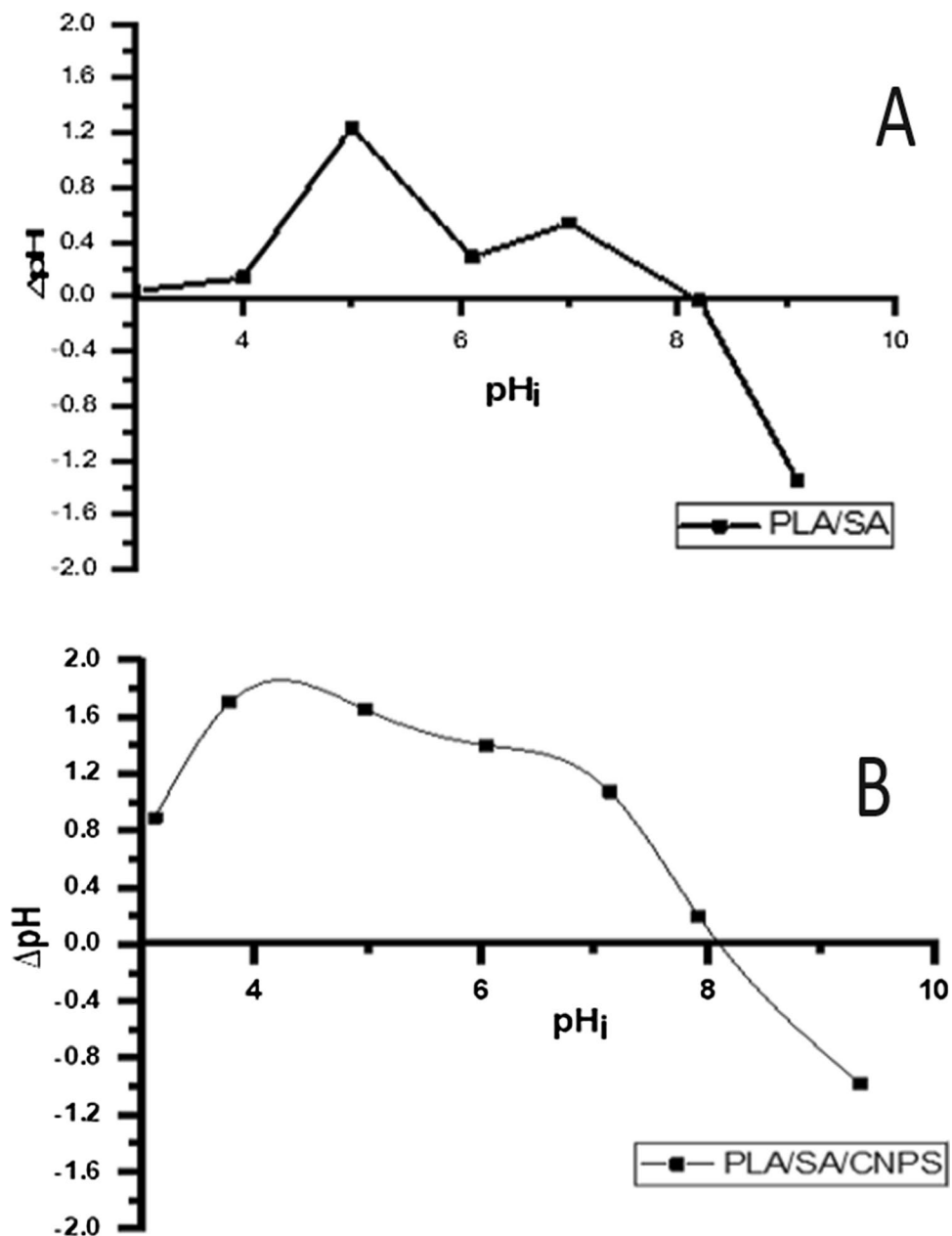
In this study, pH drift method (Badran et al. 2021) was used to find pHzpc. Using 20 mL of a 0.05 M NaCl solution for this procedure. Each solution's initial pH (pHi) was adjusted to be between (3–10) by adding 0.1 M of (NaOH or HCL). After this, 0.5 g of prepared adsorbent was placed with each solution and the mixtures was shaken at 180 rpm at 25 °C for

24 h. The final pH (pHf) of the supernatant was calculated using a pH metre. The change in pH (ΔpH) for each solution was plotted versus initial pH and the intersection point of the curve with abscissa given the value of pHzpc and it was found to be pH 8.1 for PLA/SA and PLA/SA/CNPS as shown in Fig. 7.

Effect of the addition of CNP on the main properties of the adsorbent

The addition of CNP to the polymeric matrix led to changing in the properties of the adsorbent due to CNP deposited on the granules' surface being particularly porous, offering additional potential locations for the adsorption of metal ions. Because of the alginate-activated carbon's porous structure, which provides enough surface for the adsorption of metal ions, its capacity to adsorb MB is increased.

Fig. 7 pHzpc of **a** PLA/SA and **b** PLA/SA/CNPS



Influence of CNP content on the percentage dye adsorbed of PLA/SA/CNP beads.

The percentage of dye adsorbed at the various concentrations of CNP content in the 0, 1, 3, and 5% wt was examined in the presence of 100 mg/L of MB at pH 7. The results, illustrated in Fig. 8, revealed the percentage of absorbed dye improved as CNP content increased. The surface area increases as more adsorption sites become available because of CNP's contribution to the adsorption enhancement. When the PLA/SA beads contained CNP 5% wt., the greatest percentage of sorption of PLA/SA/CNP beads at equilibrium was 98.45%. This demonstrated that a large surface area of

the adsorbent and many adsorption sites contributed to an increase in the percentage of dye adsorbed; consequently, a small increase in the amount of adsorbent provided a significantly greater surface area to absorb large numbers of MB molecules. In the literature (Ahmad et al. 2011), the same outcome has been described.

Batch study

Influence of pH

At an initial dye concentration of 100 mg/L, the influence of pH on MB dye adsorption by PLA/SA/CNP 5% wt. beads

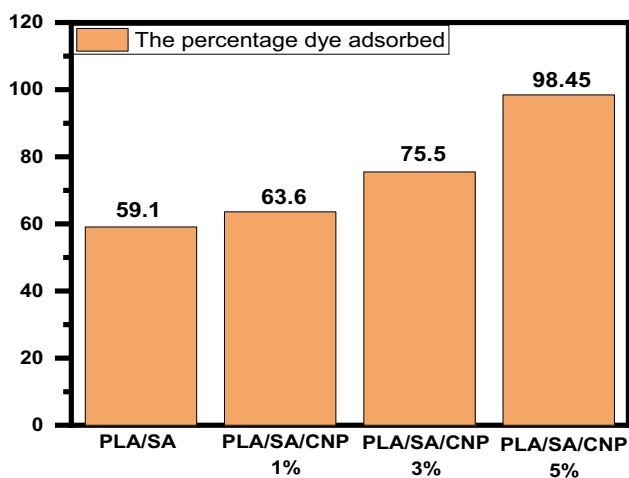


Fig. 8 Influence of CNP content (0, 1, 3 and 5% wt.) added into PLA/SA on the methylene blue adsorption

were examined in the pH range (3–9). As a cationic dye, methylene blue has a positive charge in its aqueous solutions, as seen in Fig. 2. As a result, adsorption is affected by both the charge on the surface of the beads and the medium's pH. The PLA/SA/CNP 5% wt. beads' CNP functional groups were encouraged to protonate because of the higher H^+ ion concentration, and the MB dye was repellent because of the higher total positive charge. At low pH levels, the H^+ ions compete with MB dye for adsorption sites.

When the pH is high, the surface of the beads becomes negatively charged, enhancing adsorption. Since MB is a cationic dye, the adsorption process is improved by electrostatic attraction (Aluigi, A et al.2014). Figure 9 shows that the clearance percentage increases as pH increases. This is due to the functional groups on the prepared beads having a negative charge. Additionally, at high pH levels, the rivalry between MB molecules and protons decreases. Accordingly, pH 9 was chosen as the ideal pH for investigations. Figure 9 shows the adsorbent's surface before and after it was exposed to MB dye at pH 9. The relative standard deviation (RSD) for five replicate measurements was calculated to be 0.85% for 100 mg/L (Fig. 10).

Influence of contact time

PLA/SA/CNP (5% wt.) beads were used to examine the impact of contact time (15–180 min) on the adsorption of MB dye at an initial dye concentration of 100 mg/L. The removal % of MB dye utilizing PLA/SA/CNP (5% wt) beads was dramatically increase over the first 60 min, due to the adsorbent surface having a lot of active sites, as demonstrated by the data in Fig. 11. At 120 min, the process reached equilibrium. Following that, the outside pores became saturated, which marginally enhanced the adsorption

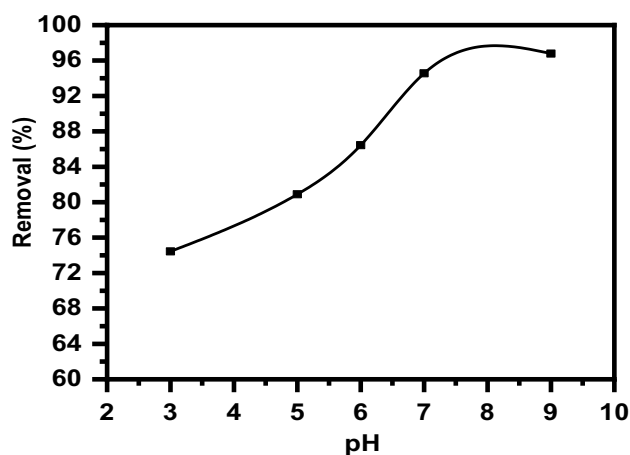


Fig. 9 The effect of pH on the MB dye's ability to bind to PLA/SA/CNP 5% wt beads (dye concentration 100 mg/L, adsorbent dosage 50 mg, contact period 120 min, temperature 25 °C)

rate, and the MB dye needed a lot of time to enter the inside pores. Therefore, it was decided that 120 min was the best contact time for studies. The relative standard deviation (RSD) for five replicate measurements was calculated to be 0.88% for 100 mg/L.

Influence of adsorbent dosage

The influence of PLA/SA/CNP 5% wt beads dosage on the elimination of 100 mg/L of MB was investigated. The PLA/SA/CNP dose is 5% wt beads ranging from 5 to 200 mg. Figure 11's results show that the percentage of MB sorption at equilibrium increased as the dosage of PLA/SA/CNP 5% wt. beads was increased. The percentage of methylene blue adsorption increased slightly at doses greater than 50 mg. This finding may be explained by the fact that even when the adsorbent dosage was raised, the amount of methylene blue molecules bound to the adsorbent and the number of free dye molecules remained unchanged. Rhodamine B is known to exhibit a comparable behavior (Hayeeye et al. 2017). The relative standard deviation (RSD) for five replicate measurements was 0.81% for 100 mg/L (Fig. 12).

Influence of concentration of adsorbate

The influence of the initial concentration of dye (50–400 mg/L) on the adsorption of MB dye is illustrated in Fig. 13. When the concentration increased from 50 to 400 mg/L, it was seen that the absorption percentage decreased from 98.54 to 72.74. The MB dye tends to bind at higher concentrations to form molecules of large sizes that cannot enter the interior pores of the adsorbent, and this is why the highest adsorption occurred at a range of (50–100 mg/L). Additionally, at high MB dye

Fig. 10 A camera images of the adsorbent both before and after adsorption (a, b)

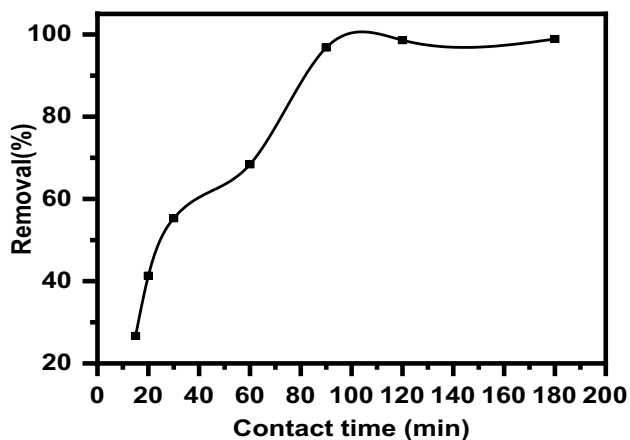
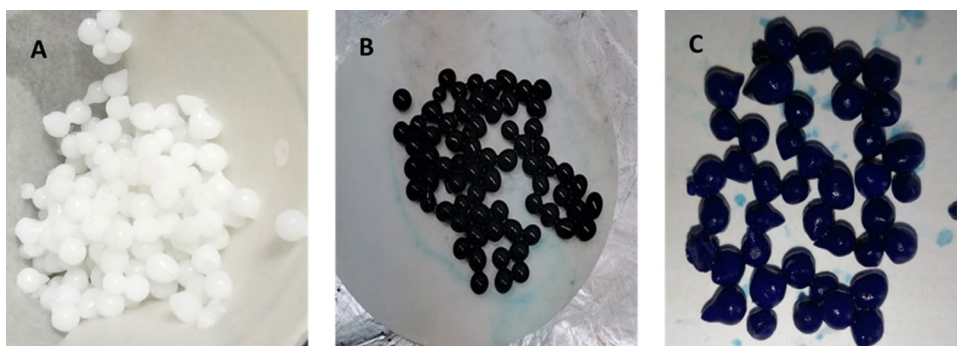


Fig. 11 Adsorption of MB dye onto PLA/SA/CNP 5% wt beads: Effect of contact time (dye concentration 100 mg/L, pH=9, adsorbent dosage 50 mg)

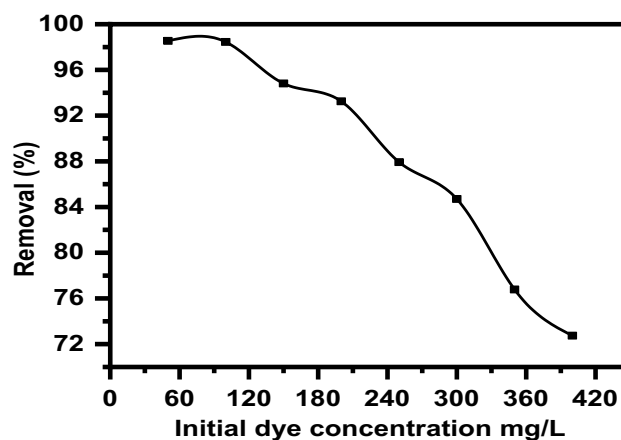


Fig. 13 Effect of dye concentration on the adsorption of MB dye onto PLA/SA/CNP beads

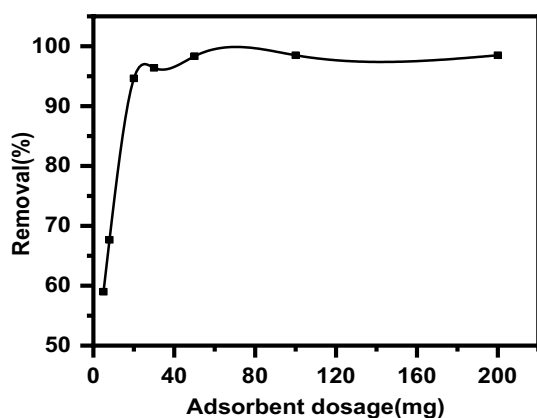


Fig. 12 Effect of the adsorbent dosage on the adsorption of MB dye onto PLA/SA/CNP 5% wt. beads [dye concentration 100 mg/L, pH=9, contact time 120 min, temperature 25 °C]

concentrations, the adsorbent surface's active sites were saturated, which decreased the removal percentage on the surface of PLA/SA/CNP5% wt. beads, as shown in Fig. 14.

The relative standard deviation (RSD) for five replicate measurements was calculated to be 0.72%.

Influence of Temperature

The effect of temperature on MB adsorption was studied at temperatures ranging from 25 to 60 °C. The results are illustrated in Fig. 15; it is noticeable that the decrease in the removal of MB by the PLA/SA/CNP beads with increasing temperature. As shown in Fig. 15, the increase in temperature from 25 to 60 °C decreases MB removal percent from 98.54 to 95%. This behavior indicates that the adsorption process is exothermic.

Isotherm study

Several models that study the adsorption isotherm curves are illustrated in the literature (A.O, 2012; Allen et al. 2004; Başar 2006). The adsorption of methylene blue solution by the manufactured beads was examined using Langmuir and Freundlich models in the current work (Allen, et al. 2004; Başar, et al. 2006; Aluigi et al. 2014). Common isotherms models that are used to determine the applicability of the

Fig. 14 The camera picture shows the effect of different dye concentrations on the removal% of MB dye onto PLA/SA/CNP 5 wt% beads, **a** before adsorption, **b** after adsorption

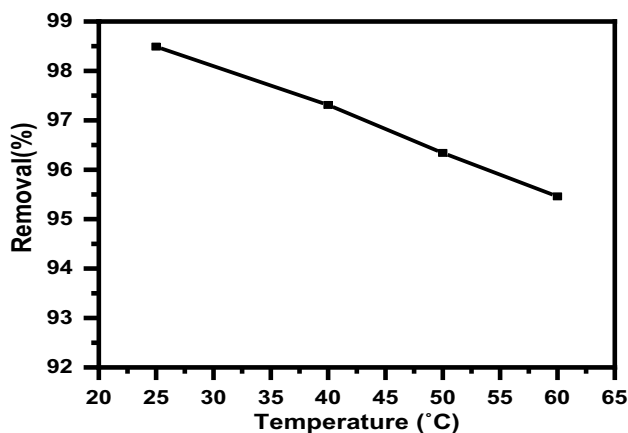
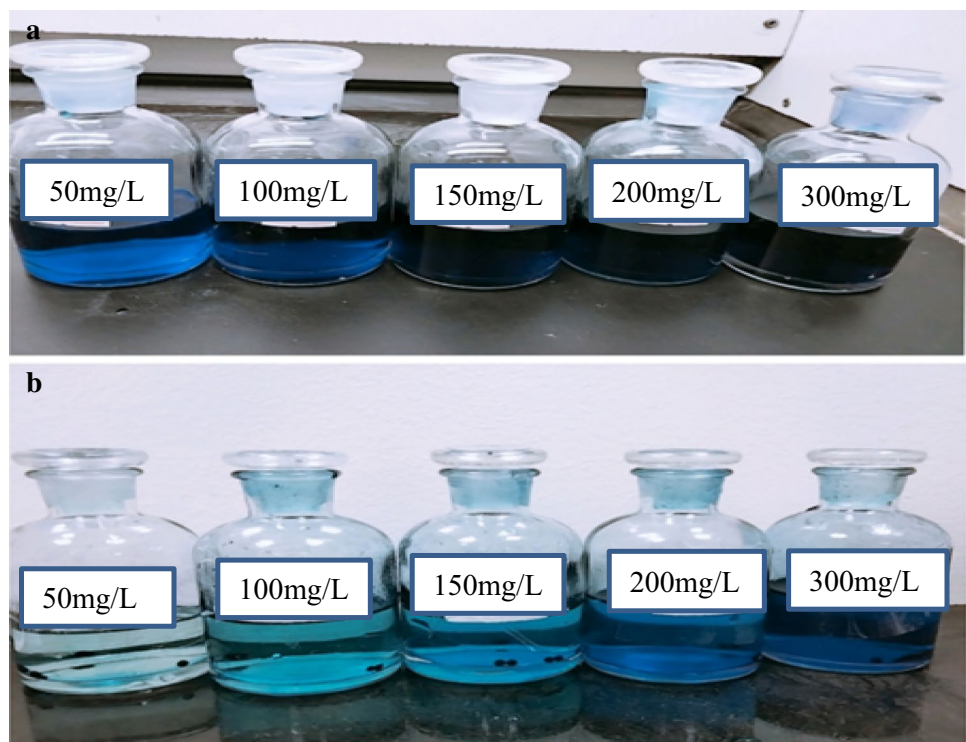


Fig. 15 Effect of temperature on the removal of MB by PLA/SA/CNP beads

adsorption process are the Langmuir's and Freundlich's models, which also reveal on the adsorption mechanism. The Langmuir model proposes that adsorption is a monolayer process (Khalil et al. 2021). The Langmuir's equation is described as follows:

$$\frac{C_e}{q_e} = \frac{1}{K_L \cdot q_{\max}} + \frac{C_e}{q_{\max}} \quad (3)$$

where C_e is MB equilibrium concentration (mg/L), q_e is the equilibrium adsorption capacity at distinct MB concentration

($\text{mg} \cdot \text{g}^{-1}$), K_L (L/mg) is Langmuir constant and q_m (mg/g) is the adsorption capacity of the prepared adsorbent. Adsorption is assumed to be a multilayer process, per Freundlich's model. The linearized form of the Freundlich equation is as follows:

$$\ln q_e = \ln K_f + \frac{1}{n} \ln C_e \quad (4)$$

KF is the Freundlich constant; $(1/n)$ is the adsorption intensity.

Figures 16 and 17 show descriptions of the Freundlich and Langmuir models, respectively. For the initial concentration of MB dye (50–400 mg/L), the equilibrium period was 120 min. Table 1 lists the estimated values of their constants (1). The data for regression coefficients R^2 showed that the Langmuir model, which has an adsorption capacity equal to 304.88 mg/g, better describes the adsorption of MB on PLA/SA/CNPS beads.

Adsorption kinetic

To investigate the rate and mechanism of MB adsorbed at equilibrium and at time t (min), respectively, and the key step of the adsorptive removal operation, experimental data were fitted by models of pseudo-first order and pseudo-second order (Hu et al. 2010; Mortada et al. 2023), which represented as following:

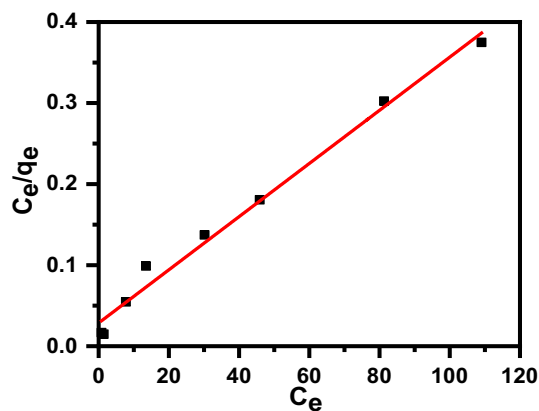


Fig. 16 Langmuir isotherm of MB dyes adsorption onto PLA/SA/CNP 5% wt. beads at 25 °C

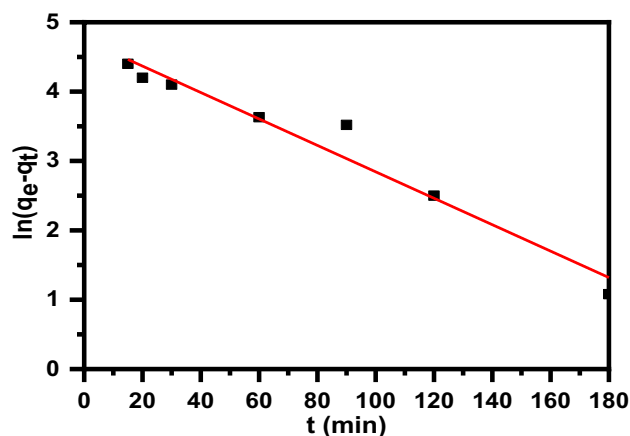


Fig. 18 pseudo-first order model of MB adsorbed on PLA/SA/CNP beads

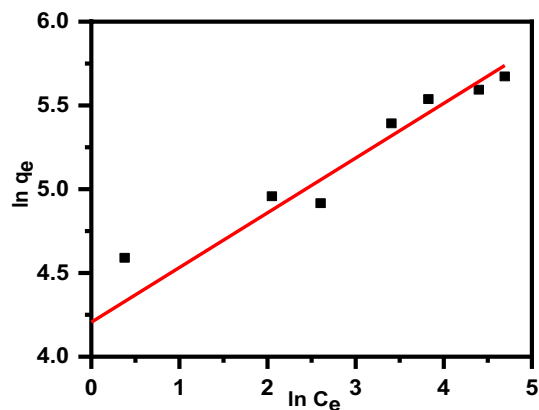


Fig. 17 Freundlich isotherm of MB dyes adsorption onto PLA/SA/CNP 5% wt. beads at 25 °C

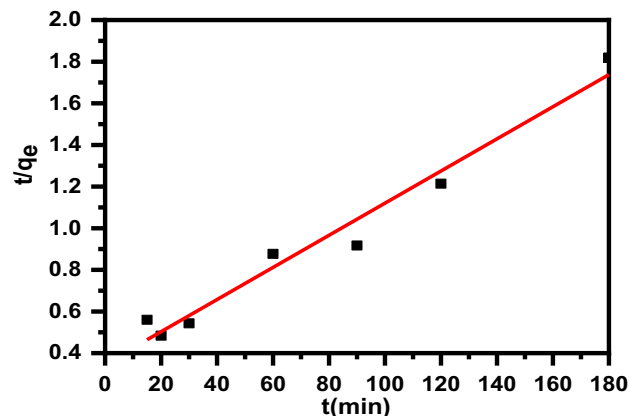


Fig. 19 pseudo-second-order model of MB adsorbed on PLA/SA/CNP beads

Table 1 Isotherm model parameters for MB dye adsorption by PLA/SA/CNP5% wt. beads at 25 °C

Adsorption isotherm	Parameter	Value
Langmuir	q_m (mg/L)	304.880
	K_L (L/mg)	0.115
	R^2	0.986
	MSE	4.80554E-33
Freundlich	n	3.062
	K_f (mg/g)	67.068
	R^2	0.952
	MSE	8.56395E-31

$$\ln(q_e - qt) = \ln q_e - K_1 t \quad (5)$$

$$t/qt = 1/K_2 q_e^2 + t/q_e \quad (6)$$

where qt (mg/g) is the adsorbed dose of CV at time t (min), q_e (mg/g) is adsorbed amount of CV at equilibration, and K_1 (min^{-1}) is the rate constant for pseudo-first order, K_2 ($\text{g}/\text{mg}\cdot\text{min}$) is the rate constant for pseudo-second order.

Figures 18 and 19 represent the experimental data and the curve-fitting results are compiled in Table 2. From values of correlation coefficient (R^2), the pseudo-second order was better than the pseudo-first order which suggested that the adsorption of MB onto the adsorbent surface obeys the pseudo-second-order model and there is a strong force between the adsorbent surface and adsorbate caused by surface complexation of MB with the functional groups on the surface of the adsorbent. Also, the pseudo-second-order model suggests that the rate-controlling step is chemisorption in the adsorption process (Ahmed & Ahmed 2015).

Table 2 Showed kinetic models and their parameters in the adsorption of MB on PLA/SA/CNP beads

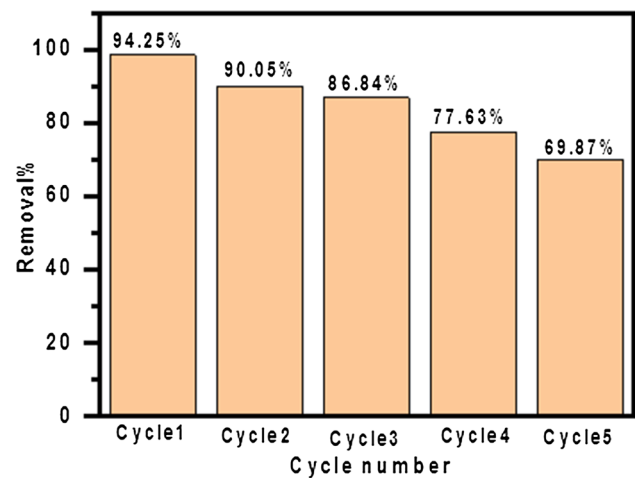
Kinetic model	Parameter	Value
Pseudo-first order (PFO)	Q_e (mg/g)	114.43
	K_1 (min) ⁻¹	0.019
	R^2	0.952
Pseudo-second order (PSO)	Q_e (mg/g)	129.53
	K_2 (g/mg.min)	0.00017
	R^2	0.963

Regeneration study

The feasibility of reusing the beads will be investigated for both environmental and financial reasons. The produced beads were soaked in a 1 M HCl solution for 15 min before being filtered and thoroughly dried. The tested MB solution had 100 mg/L of dye, 50 mg of adsorbent, a pH of 9, and a contact duration of 120 min at a temperature of 25 °C. We achieved five adsorption–desorption cycles. PLA/SA/CNP 5% wt. beads' surface had adsorbed MB dye removed using HCl after each cycle. Figure 20 shows the outcome and illustrates how less MB dye was eliminated as a result. This is due to the surface of the beads losing part of their active regions. So, following the fifth cycle, adsorption efficiency dropped by 28.58%.

The suggested mechanism for the adsorption process.

A proposed process for the adsorption of MB dye onto PLA/SA/CNP is shown in Fig. 21. Carboxyl groups are present on the surface of SA and CNP similarly. Therefore, the formation of the PLA/SA/CNP is achieved via a strong hydrogen bond between SA and CNP. Adsorption tests (impact of solution pH) revealed that at pH 9, a high level of MB adsorption onto the PLA/SA/CNP surface was accomplished. This finding refers to a powerful electrostatic interaction between

**Fig. 20** Removal efficiency of PLA/SA/CNP 5% wt. Beads in a five successive adsorption–desorption cycle process

the molecules of the MB dye and the adsorbent. This result refers to a powerful electrostatic interaction between the molecules of the MB dye and the adsorbent. The surface of PLA/SA/CNP had a lot of carboxyl groups, which dissociated into carboxylate anions, that influenced the attraction of positively charged MB dye molecules. The strong adsorption capacity of PLA/SA/CNP may also be due to the π - π stacking interaction between MB onto CNP.

Comparison with different adsorbents.

This study indicates that PLA/SA/CNP beads have great potential as an effective matrix for removing the methylene blue dye from aqueous solutions. We find that the new matrix is more effective and superior to the previously used materials in removing the dye when compared to the results previously published, which are shown in Table 2. This finding suggests that the new matrix can be used as an efficient method to remove MB dye after further development in the future at the industrial level (Table 3).

Table 3 The adsorbent's MB adsorption capacity is compared to that of other adsorbents previously reported

Adsorbents	Qmax (mg/g)	Refs
keratin nanofibers	170.0	Aluigi et al. 2014
PVP/PCMC/GO/bentonite hydrogel	172.1	Dai et al. 2018
Polydopamine-coated electrospun poly(vinyl alcohol)/poly(acrylic acid)	180.0	Yan et al. 2015
Magnetic PVA/Iaponite RD hydrogel nanocomposite	251.0	Mahdavinia, et al. 2017
Nanocomposite of chitosan/silica/ZnO	293.3	Hassan et al. 2019
Ho-CaWO4	103.09	(Igwegbe et al. 2019)
Amberlite resin supported GO	155.25	(Çiğeroğlu et al. 2020)
1.0% g-C3N4/CNCs-H hydrogel	232.55	(Wang et al. 2020)
poly(β -CD-BPDA)	96.15	(Lagiewka et al. 2023)
PLA/SA/CNP beads	304.88	Current study

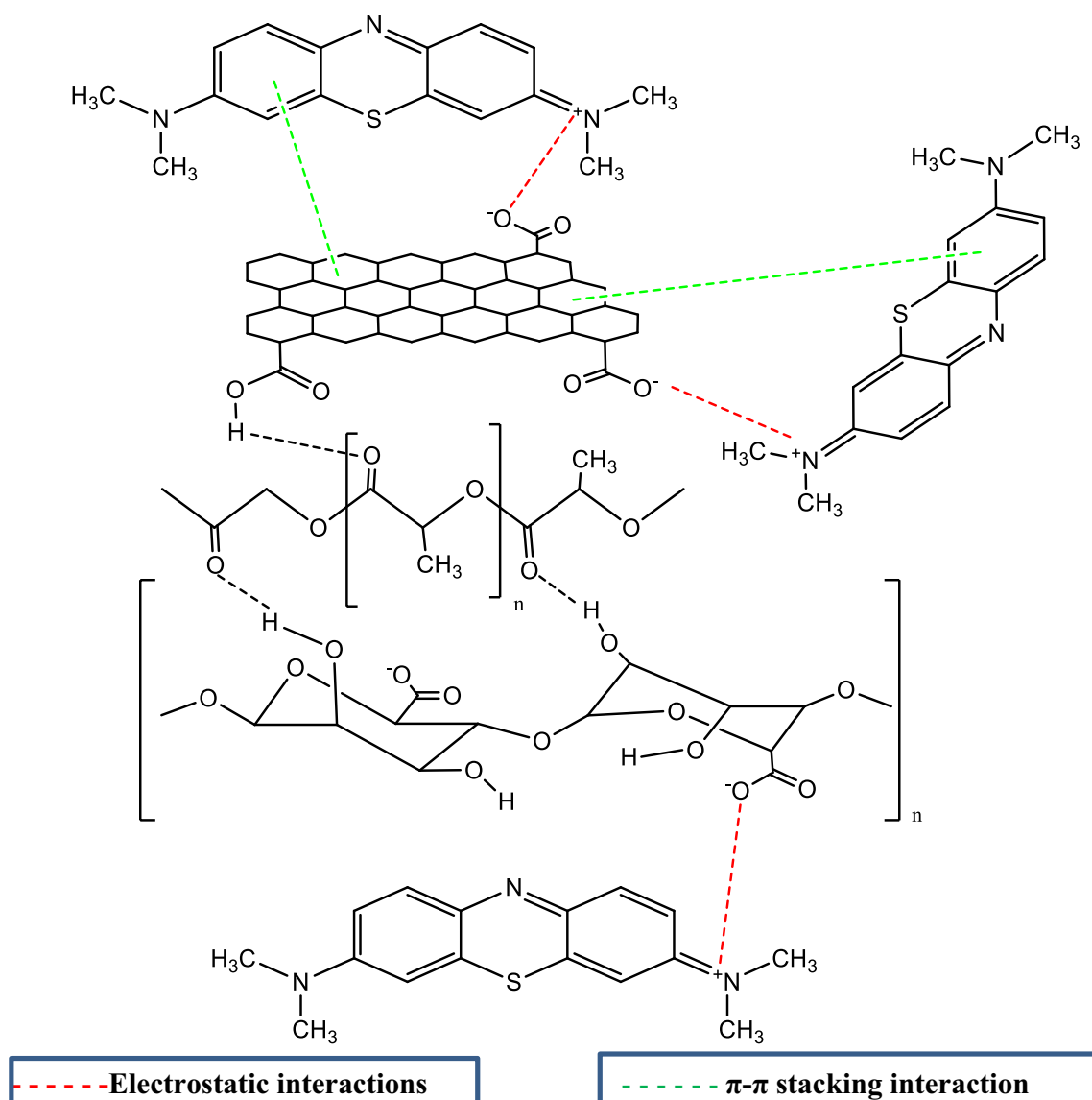


Fig. 21 The suggested adsorption mechanism of MB dye on PLA/SA/CNP beads

Conclusion

For the adsorption of methylene blue (MB), novel biopolymeric matrices prepared from polylactic acid/sodium alginate (PLA/SA) and polylactic acid/sodium alginate/carbon nanoparticle (PLA/SA/CNP) as green adsorbates were prepared in the form of beads.

In this work, PLA/SA and (PLA/SA/CNP) beads were prepared for the successful adsorption of methylene blue (MB) dye. The amount of adsorbent used, the starting pH, the contact period, and the dye concentration all had an impact on the amount of MB that removed by the adsorbent. pH 9, 50 mg of the adsorbent and a contact period of 120 min with an initial dye concentration of 100 mg/L were the optimal working conditions. The Langmuir model

fits the equilibrium data well with 304.88 mg/g capacity of adsorption. Functional groups on the surface of PLA/SA/CNP, such as (–OH) and (–COO–), are responsible for MB dye's binding to the PLA/SA/CNP surface, according to the FTIR spectroscopy investigations. The regeneration study was applied using HCl (1 M) remarkably after the fifth cycle; the percentage removal loss was only 28.58%. This study indicates that PLA/SA/CNP beads have exciting potential for cationic methylene blue dye removal from aqueous solutions.

Funding Open access funding provided by The Science, Technology & Innovation Funding Authority (STDF) in cooperation with The Egyptian Knowledge Bank (EKB).

Data availability The datasets used and/or analyzed during the current study are available from the corresponding author on reasonable request.

Declarations

Conflict of interest The authors declare no conflict of interests.

Open Access This article is licensed under a Creative Commons Attribution 4.0 International License, which permits use, sharing, adaptation, distribution and reproduction in any medium or format, as long as you give appropriate credit to the original author(s) and the source, provide a link to the Creative Commons licence, and indicate if changes were made. The images or other third party material in this article are included in the article's Creative Commons licence, unless indicated otherwise in a credit line to the material. If material is not included in the article's Creative Commons licence and your intended use is not permitted by statutory regulation or exceeds the permitted use, you will need to obtain permission directly from the copyright holder. To view a copy of this licence, visit <http://creativecommons.org/licenses/by/4.0/>.

References

- AO D (2012) Langmuir, freundlich, temkin and dubinin-radushkevich isotherms studies of equilibrium sorption of Zn²⁺ onto phosphoric acid modified rice husk. *IOSR J Appl Chem* 3(1):38–45. <https://doi.org/10.9790/5736-0313845>
- Ahmed E, Ahmed M (2015) By Supervised by Prof. Dr. Mohamed Mohamed El-Defrawy Dr. Hany Moustafa Youssef Dr. Eman Hamed Abo El-Nadar. 2021.
- Ali KA, Hassan ME, Elnashar MMM (2017) Development of functionalized carrageenan, chitosan and alginate as polymeric chelating ligands for water softening. *Int J Environ Sci Tech* 14(9):2009–2014. <https://doi.org/10.1007/s13762-017-1298-y>
- Allen SJ, McKay G, Porter JF (2004) Adsorption isotherm models for basic dye adsorption by peat in single and binary component systems. *J Colloid Interface Sci* 280(2):322–333. <https://doi.org/10.1016/j.jcis.2004.08.078>
- Aluigi A, Rombaldoni F, Tonetti C, Jannoke L (2014) Study of Methylene Blue adsorption on keratin nanofibrous membranes. *Journal of Hazardous Materials*, 268:156–165. <https://doi.org/10.1016/j.jhazmat.2014.01.012>
- Amin K A, Abdel Hameid H, Abd Elsttar A H (2010) Effect of food azo dyes tartrazine and carmoisine on biochemical parameters related to renal, hepatic function and oxidative stress biomarkers in young male rats. *Food and Chemical Toxicology* 48(10):2994–2999. <https://doi.org/10.1016/j.fct.2010.07.039>
- Annadurai G, Chellapandian M, Krishnan M R V (1999) Adsorption of reactive dye on chitin. *Environmental Monitoring and Assessment* 59(1):111–119. <https://doi.org/10.1023/A:1006072119624>
- Ayad M M, El-Nasr A A (2012) Anionic dye (acid green 25) adsorption from water by using polyaniline nanotubes salt/silica composite. *Journal of Nanostructure in Chemistry* 3(1):1–9 <https://doi.org/10.1186/2193-8865-3-3>
- Badran EA, Youssef HM, El-Defrawy MM (2021) Exploitation of an agro-industrial waste in eco-friendly clean-up: adsorptive removal of Congo red dye from aqueous media using chemically treated olive pomace. *Int J Environ Anal Chem* 00(00):1–20. <https://doi.org/10.1080/03067319.2021.1931156>
- Başar CA (2006) Applicability of the various adsorption models of three dyes adsorption onto activated carbon prepared waste apricot. *J Hazard Mater* 135(1–3):232–241. <https://doi.org/10.1016/j.jhazmat.2005.11.055>
- Çiğeroğlu Z, Küçükyıldız G, Haşimoğlu A, Taktak F, Açıköz N (2020) Fast and effective methylene blue adsorption onto graphene oxide/amberlite nanocomposite: Evaluation and comparison of optimization techniques. *Korean J Chem Eng* 37(11):1975–1984. <https://doi.org/10.1007/s11814-020-0600-8>
- Crini G, Badot PM (2008) Application of chitosan, a natural aminopolysaccharide, for dye removal from aqueous solutions by adsorption processes using batch studies: a review of recent literature. *Prog Polym Sci (Oxford)* 33(4):399–447. <https://doi.org/10.1016/j.progpolymsci.2007.11.001>
- Dai H, Huang Y, Huang H (2018) Eco-friendly polyvinyl alcohol/carboxymethyl cellulose hydrogels reinforced with graphene oxide and bentonite for enhanced adsorption of methylene blue. *Carbohydr Polym* 185:1–11. <https://doi.org/10.1016/J.CARBPOL.2017.12.073>
- Hassan H, Salama A, El-ziaty AK, El-Sakhawy M (2019) New chitosan/silica/zinc oxide nanocomposite as adsorbent for dye removal. *Int J Biol Macromol* 131:520–526. <https://doi.org/10.1016/j.ijbiomac.2019.03.087>
- Hayeey F, Sattar M, Chinpa W, Sirichote O (2017) Kinetics and thermodynamics of Rhodamine B adsorption by gelatin/activated carbon composite beads. *Colloids and Surfaces A: Physicochemical and Engineering Aspects* 513:259–266. <https://doi.org/10.1016/j.colsurfa.2016.10.052>
- Ho CS, Abidin NHZ, Nugraha MW, Sambudi NS, Ali F, Wirzal MDH, Kasmirno LD, Adli SA (2020) Electrospun porous polylactic acid fibers containing CdS for degradation of methylene blue. *Fibers and Polymers* 21(6):1212–1221. <https://doi.org/10.1007/s12221-020-9756-4>
- Hu T, Liu Q, Gao T, Dong K, Wei G, Yao J (2018) Facile Preparation of Tannic Acid-Poly(vinyl alcohol)/Sodium Alginate Hydrogel Beads for Methylene Blue Removal from Simulated Solution. *ACS Omega* 3(7):7523–7531. https://doi.org/10.1021/ACSOMEGA.8B00577/SUPPL_FILE/AO8B00577_SI_001.PDF
- Hu X, Li Y, Wang Y, Li X, Li H, Liu X, Zhang P (2010) Adsorption kinetics, thermodynamics and isotherm of thiocalix[4]arene-loaded resin to heavy metal ions. *Desalination* 259(1–3):76–83. <https://doi.org/10.1016/J.DESAL.2010.04.032>
- Igwegbe CA, Mohmmadi L, Ahmadi S, Rahdar A, Khadkhodaiy D, Dehghani R, Rahdar S (2019) Modeling of adsorption of methylene blue dye on Ho-CaWO₄ nanoparticles using response surface methodology (RSM) and artificial neural network (ANN) techniques. *MethodsX* 6:1779–1797. <https://doi.org/10.1016/J.MEX.2019.07.016>
- Kaushal M, Tiwari A (2010) Removal of rhodamine-b from aqueous solution by adsorption onto crosslinked alginate beads. *J Dispers Sci Tech* 31(4):438–441. <https://doi.org/10.1080/01932690903210135>
- Khalil U, Shakoob MB, Ali S, Ahmad SR, Rizwan M, Alsahli AA, Alyemeni MN (2021) Selective removal of hexavalent chromium from wastewater by rice husk: Kinetic, isotherm and spectroscopic investigation. *Water (switzerland)* 13(3):263. <https://doi.org/10.3390/w13030263>
- Koumanova B, Allen SJ (2005) Decolourisation of Water/Wastewater using adsorption (review). *J Univ Chem Tech Metall* 40:175–192
- Labena A, Abdelhamid AE, Amin AS, Husien S, Hamid L, Safwat G, Diab A, Gobouri AA, Azab E (2021) Removal of methylene blue and congo red using adsorptive membrane impregnated with dried ulva fasciata and sargassum dentifolium. *Plants* 10(2):1–26. <https://doi.org/10.3390/plants10020384>
- Lagiewka J, Nowik-Zajac A, Pajdak A, Zawierucha I (2023) A novel multifunctional β -cyclodextrin polymer as a promising sorbent for rapid removal of methylene blue from aqueous solutions. *Carbohydrate Polym* 307:120615. <https://doi.org/10.1016/J.CARBOL.2023.120615>

- Li PG, Bono A, Krishnaiah D, Collin JG (2008) Preparation of titanium dioxide photocatalyst loaded onto activated carbon support using chemical vapor deposition: a review paper. *J Hazard Mater* 157(2–3):209–219. <https://doi.org/10.1016/j.jhazmat.2008.01.040>
- Makhado E, Hato MJ (2021) Preparation and Characterization of Sodium Alginate-Based Oxidized Multi-Walled Carbon Nanotubes Hydrogel Nanocomposite and its Adsorption Behaviour for Methylene Blue Dye. *Frontiers in Chemistry*, 9(March) 1–16. <https://doi.org/10.3389/fchem.2021.576913>
- McKay G, Ramprasad G, Pratapa Mowli P (1986) Equilibrium studies for the adsorption of dyestuffs from aqueous solutions by low-cost materials. *Water, Air, and Soil Pollution* 29(3):273–283. <https://doi.org/10.1007/BF00158759>
- Mohammad N, Atassi Y (2020) Adsorption of methylene blue onto electrospun nanofibrous membranes of polylactic acid and polyacrylonitrile coated with chloride doped polyaniline. *Sci Rep* 10(1):1–19. <https://doi.org/10.1038/s41598-020-69825-y>
- Mortada WI, Mohamed RA, Monem AAA, Awad MM, Hassan AF (2023) Effective and Low-Cost Adsorption Procedure for Removing Chemical Oxygen Demand from Wastewater Using Chemically Activated Carbon Derived from Rice Husk. *Separations* 10(1):43. <https://doi.org/10.3390/separations10010043>
- Sabarinathan C, Karuppasamy P, Vijayakumar CT, Arumuganathan T (2019) Development of methylene blue removal methodology by adsorption using molecular polyoxometalate: Kinetics. *Thermodyn Mech Study Microchem J* 146(2018):315–326. <https://doi.org/10.1016/j.microc.2019.01.015>
- Salisu A, Sanagi MM, Naim AA, Karim KJ (2015) Removal of methylene blue dye from aqueous solution using alginate grafted polyacrylonitrile beads. *Der Pharma Chemica* 7(2):237–242
- Sattar M, Hayeeye F, Chinpa W, Sirichote O (2017) Preparation and characterization of poly (lactic acid)/activated carbon composite bead via phase inversion method and its use as adsorbent for Rhodamine B in aqueous solution. *J Environ Chem Eng* 5(4):3780–3791. <https://doi.org/10.1016/j.jece.2017.07.007>
- Soleimani S, Heydari A, Fattahi M, Motamedisade A (2023) Calcium alginate hydrogels reinforced with cellulose nanocrystals for methylene blue adsorption: Synthesis, characterization, and modelling. *Ind Crops Prod* 192:115999. <https://doi.org/10.1016/j.indcrop.2022.115999>
- Song X, Zhou J, Fan J, Zhang Q, Wang S (2022) Preparation and adsorption properties of magnetic graphene oxide composites for the removal of methylene blue from water. *Mater Res Exp* 9(2):159. <https://doi.org/10.1088/2053-1591/ac52c6>
- Sumanjit WT, Kaur R (2007) Removal of health hazards causing acidic dyes from aqueous solutions by the process of adsorption. *Online J Health Allied Sci* 6(3)
- Wan NWS, Teong LC, Hanafiah MAKM (2011) Adsorption of dyes and heavy metal ions by chitosan composites: a review. *Carbohydr Polym* 83(4):1446–1456. <https://doi.org/10.1016/j.carbpol.2010.11.004>
- Wang H, Li J, Ding N, Zeng X, Tang X, Sun Y, Lei T, Lin L (2020) Eco-friendly polymer nanocomposite hydrogel enhanced by cellulose nanocrystal and graphitic-like carbon nitride nanosheet. *Chem Eng J* 386:124021. <https://doi.org/10.1016/J.CEJ.2020.124021>
- Yan J, Huang Y, Miao YE, Tjiu WW, Liu T (2015) Polydopamine-coated electrospun poly(vinyl alcohol)/poly(acrylic acid) membranes as efficient dye adsorbent with good recyclability. *J Hazard Mat* 283:730–739. <https://doi.org/10.1016/j.jhazmat.2014.10.040>

Publisher's Note Springer Nature remains neutral with regard to jurisdictional claims in published maps and institutional affiliations.